Effects of spatial inhomogeneities on the dynamics of cavity solitons in quadratically nonlinear media

S. Fedorov,[1] D. Michaelis,[2] U. Peschel,[2] C. Etrich,[2] D. V. Skryabin,[3] N. Rosanov,[1] and F. Lederer[2]
[1]*Institute for Laser Physics, Vavilov State Optical Institute, Birzhevaya line 12, 199034 St. Petersburg, Russia*
[2]*Friedrich-Schiller-Universität Jena, Max-Wien-Platz 1, 07743 Jena, Germany*
[3]*Department of Physics and Applied Physics, University of Strathclyde, Glasgow G4 0NG, United Kingdom*
(Received 19 March 2001; published 29 August 2001)

We study the dynamics of cavity solitons under the influence of spatial inhomogeneities and derive generalized equations of motions. For perturbations large compared to the soliton size we find the modulus of the soliton velocity to be proportional to the gradient of the respective perturbation and that the proportionality coefficient changes sign when the soliton peak power drives the cavity beyond the resonance. For short scale perturbations solitons may be trapped at the extrema of the inhomogeneities. Shape and stability of these trapped solitons can be quasianalytically described by means of a perturbation theory. If both types of perturbations act solitons are either trapped or move depending on the strength of the respective perturbation. In the framework of a quasiparticle approach this dynamics is governed by a differential equation that holds for particle motion in a strongly viscous fluid under the action of a constant and harmonically varying force. We also show that in addition to acquiring a velocity the very existence conditions of the solitons (hysteresis curve) are affected by both kinds of perturbations. We find good quantitative agreement between our analytical results and numerical findings, which were obtained for a two wave interaction in a cavity filled with a quadratically nonlinear material.

DOI: 10.1103/PhysRevE.64.036610 PACS number(s): 42.65.Tg, 42.65.Ky, 42.65.Sf

I. INTRODUCTION

Cavity solitons (CSs) were predicted to exist in externally driven wide-aperture nonlinear interferometers or Fabry-Perot resonators [1,2]. Here the effects of different types of intensity-dependent nonlinearities, such as saturable absorptive [3], focusing dispersive [4], saturable focusing [1,5,6] or semiconductor ones [7,8] were investigated. In the limit of nascent bistability in the presence of modulational instability nonlinear systems can be often reduced to the Swift-Hohenberg equation. This order parameter equation exhibits bright and dark solitary wave solutions [9]. For a Kerr nonlinearity with self- and cross-phase modulation CSs can form as a result of symmetry breaking of the polarization state [10]. Much effort has been spent on the experimental verification of these CSs in various systems. A first evidence for localized structures in nonlinear resonators was published in the mid-nineties [11–13]. Later on CSs could be identified in lasers with saturable absorbers [14,15] or degenerate optical parametric mixing [16]. Interesting for applications are promising results on CSs in semiconductor microresonators [17,18]. It has to be emphasized that CSs share a lot of common features, as, e.g., similar evolution equations, with localized structures found in other dissipative optical systems, where feedback is not necessarily induced by a cavity. Localized structures were observed in such configurations with a liquid crystal light valve [19], binary phase slices [20], and sodium cells [21].

For a given set of parameters only a limited number of localized structures with well-defined properties exists in a cavity. This is in contrast to whole families of solitons in conservative systems. Due to their definite shape and robustness CSs are promising candidates for applications in optical information storage and processing schemes. Thus it is worthwhile to study their dynamical properties and in particular their ability to react upon external perturbations, e.g., system parameter variations. Such inhomogeneities can be used to control the position of CSs [3,22], to steer them to the point of operation or even to construct all-optical shift registers [23] and full adders [24]. It was found that smooth inhomogeneities force the cavity soliton to move into the transverse direction with a velocity proportional to the local gradient of the corresponding inhomogeneity [3,14,21,25], thus obeying a sort of ''Aristotelian mechanics'' [26]. The almost immediate convergence to a state with a defined velocity makes this concept particularly interesting for a precise signal steering or routing.

Practically relevant solutions require large and fast nonlinearities to reduce power requirements and cope with high repetition rate of the addressing pulses. A promising approach is the use of materials with quadratic nonlinearity [27]. Recently coupled localized states of light at the fundamental frequency (FF) and corresponding second harmonic (SH) frequency were predicted to exist in intracavity second harmonic generation [28–31] and optical parametric oscillators [32–40]. The goal of the present paper is to formulate dynamical laws governing the motion of the center of mass of CSs and to study limits of the ''quasiparticle'' approach. All the numerical investigations are concentrated on cavities filled with quadratically nonlinear materials. However, similar phenomena are expected to occur in the presence of other types of nonlinearities.

As we will demonstrate, CSs respond almost locally on variations of the system parameters. Therefore the finite size of the physical system as well as the particular type of boundary conditions, which were chosen to simulate the dynamical response, play a minor role. As far as the CS does not touch the boundaries during its evolution the diameter of the cavity can be regarded to be infinite. In particular cases we have modeled the finite extent of the physical system by

a Gaussian holding beam. A detailed analytical study of CSs close to system boundaries is beyond the scope of our paper.

II. EQUATIONS AND THEIR SYMMETRY

Mean field equations for a cavity with a quadratic nonlinearity were derived in [41–43]. The appropriately scaled evolution equations for the FF and SH envelopes A and B are

$$i\frac{\partial A}{\partial t}+\nabla_\perp^2 A+(i\gamma_A+\Delta_A)A+A^*B=E,$$
$$i\frac{\partial B}{\partial t}+\alpha\vec{\nabla}_\perp^2 B+(i\gamma_B+\Delta_B)B+A^2=0, \tag{1}$$

where $\nabla_\perp^2=\partial_x^2+\partial_y^2$ is the transverse Laplacian, $\gamma_{A,B}$ are the cavity decay rates at the FF and SH frequencies, $\Delta_{A,B}$ are the frequency detunings of the external (holding) field E from the cavity resonances, and α is the ratio of the effective diffraction at the FF and SH frequencies. For more details about the scaling see [43].

In principle, due to inhomogeneities of the pump profile, defects and/or curvature of mirrors and defects in nonlinear material, all parameters in Eqs. (1) can depend on the transverse coordinates x and y. In an ideal case, however, which will be used as a zero approximation in the perturbation theory developed below, one can assume that all parameters are x and y independent. Then Eqs. (1) are translationally invariant, which means that the linear spectrum of any stationary solution $(A_0(x,y),B_0(x,y))$ contains a zero-frequency Goldstone mode generated by the infinitesimal space translations and given by the gradient of the solution itself.

If the frequency of the incident field is shifted, $E=\overline{E}e^{-i\omega t}$, the transmitted fields A and B react in a similar way. The parameters of Eqs. (1) transform according to

$$\Delta_A'=\Delta_A+\omega,\quad \Delta_B'=\Delta_B+2\omega,\quad x'=x,\quad t'=t,$$
$$A'=Ae^{i\omega t},\quad B'=Be^{2i\omega t}. \tag{2}$$

For the most realistic case $\alpha=1/2$ also spatial phase gradients of the holding beam can be removed. If the holding beam is tilted by an angle θ into x direction, i.e., $E=\overline{E}e^{i\theta x}$, the cavity soliton starts to move. The exact transformation of Eqs. (1) into a moving reference frame becomes

$$\Delta_A'=\Delta_A-\theta^2,\quad \Delta_B'=\Delta_B-2\theta^2,\quad x'=x-2\theta t,$$
$$t'=t,\ \ A'=Ae^{-i\theta x},\ \ B'=Be^{-2i\theta x}. \tag{3}$$

Thus oblique incidence immediately induces a transverse motion of the fields with a velocity proportional to the tilt angle θ.

From now on we suppose $\alpha=\frac{1}{2}$ because α only slightly deviates from that value in realistic configurations. Note that oblique incidence already can be treated as the case of an E with a phase inhomogeneity that can be used to steer cavity solitons into a desired direction.

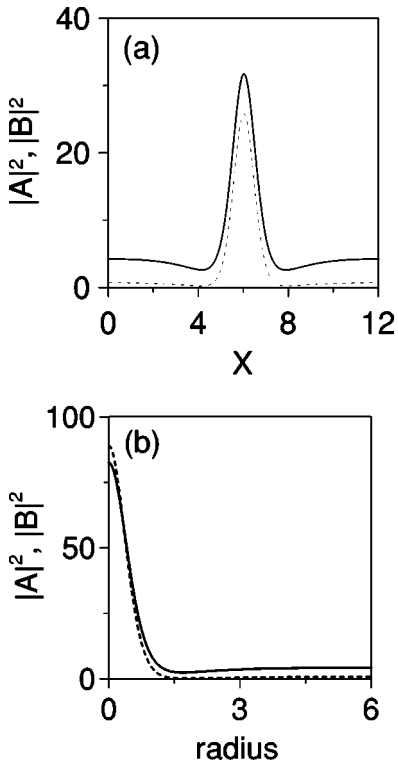

FIG. 1. Amplitudes of (a) one-dimensional and (b) two-dimensional cavity solitons due to a quadratic nonlinearity for $\Delta_A=-3$, $\Delta_B=-5$, $\gamma_A=1$, $\gamma_B=0.5$, and $E=5$.

III. QUADRATIC CAVITY SOLITONS WITH HOMOGENEOUS HOLDING FIELD

Quadratic cavity solitons exist both in one- and two-dimensional geometries, see [28–31] and Fig. 1, for an example. Usually the peak intensity is higher for two-dimensional than for one-dimensional solitons. This can be understood in an effective cubic limit. If diffraction of the SH wave can be neglected the process of subsequent up- and down-conversion generates a phase shift of the FF wave, which is similar to the one produced by a cubic nonlinearity. In the presence of a cubic nonlinearity two-dimensional beams tend to collapse, whereas one-dimensional field distributions are stable. Consequently in the presence of a quadratic nonlinearity much more energy is accumulated in the center of a two-dimensional CS than in that of an one-dimensional one. Note that the collapse is easily eliminated by the combined action of losses and quadratic nonlinearity. For both dimensions the parameter domain, where cavity solitons exist is limited, which imposes natural restrictions on the spatial variations of the system parameters. For instance, large scale variations of the holding intensity should not exceed the limit points of the hysteresis loops of the respective cavity solitons [see Fig. 2(a)]. These hysteresis loops can be determined as a function of the input intensity. For example, increasing the control parameter E (assumed to be a constant) the continuous wave (cw) solution destabilizes at one limit point and stabilizes again at the other one (homogeneous stability). For high holding beam intensities no

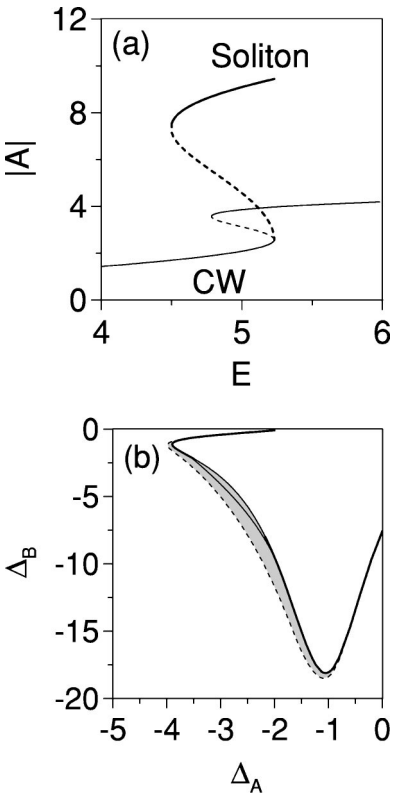

FIG. 2. (a) Hysteresis loops of cw (thin lines) and cavity solitons (bold lines) for $\Delta_A=-3$, $\Delta_B=-5$, $\gamma_A=1$, and $\gamma_B=0.5$. Solid and dashed lines refer to stable and unstable solutions, respectively. (b) Domain of existence of cavity solitons in the (Δ_A,Δ_B) plane for $E=4.5$ and $\gamma=0.5$. The bold solid line marks points where the modulational instability of cw sets in, the thin solid line limit points of branches of cw and the dashed line limit points of branches of cavity solitons.

stable low intensity background exists and therefore no solitons can be excited.

IV. DYNAMICS OF CAVITY SOLITONS UNDER THE ACTION OF LINEAR AND PERIODIC PERTURBATIONS

A. Large scale perturbations: Linear approximation

Figure 2(b) displays an example of the domain in the (Δ_A,Δ_B) plane, where cavity solitons exist for a given holding amplitude. A respective shift of the effective detuning induced by a tilt of the incident beam with an angle θ according to Eq. (3) should not cause the soliton to leave its domain of existence. Hence to allow for steering operation with a maximum gradient the point of operation should be placed at maximum values of the FF and SH detuning. For the case displayed in Fig. 2(b) any phase tilt exceeding $\theta_{\max}=0.52$ would destroy the soliton.

The response of the soliton on other inhomogeneities cannot be deduced in a straightforward way as for phase gradients. To determine the response of the soliton to the applied gradient we develop a variant of the perturbation theory assuming that position of the soliton varies adiabatically in time, which makes perturbation expansion free from the terms with polynomial growth in time. To this end we switch to a real basis rewriting Eqs. (1) in the following general form

$$\partial_t\vec{u}-\vec{w}|_{\vec{u}}=-\sum_i \delta_i\vec{P}_i x, \tag{4}$$

where we defined $\vec{u}(x)=(\mathrm{Re}\,A,\mathrm{Im}\,A,\mathrm{Re}\,B,\mathrm{Im}\,B)^T$, $\vec{w}$ is a vector that is a nonlinear function of the fields and $\Sigma_i\delta_i\vec{P}_i x$ is a gradient perturbation applied in x direction. The small quantity δ_i describes the strength of the gradient perturbation. Below, we will develop a theory, which covers both one- and two-dimensional solitons. However, for the sake of simplicity the spatial dependence of the perturbations is restricted to the x variable. Therefore all dynamics considered below will be one dimensional. For the different perturbations the vector $\vec{P}_i$ has to be chosen accordingly:

$$\begin{aligned}
&\vec{P}_E=(0,1,0,0)^T, && \text{gradient in the incidient field,}\\
&\vec{P}_{\Delta_1}=(\mathrm{Im}\,A,-\mathrm{Re}\,A,0,0), && \text{gradient in the FF detuning,}\\
&\vec{P}_{\Delta_2}=(0,0,\mathrm{Im}\,B,-\mathrm{Re}\,B), && \text{gradient in the SH detuning,}\\
&\vec{P}_{\gamma_1}=(\mathrm{ReA},\mathrm{Im}\,A,0,0), && \text{gradient in the FF loss,}\\
&\vec{P}_{\gamma_2}=(0,0,\mathrm{Re}\,B,\mathrm{Im}\,B), && \text{gradient in the SH loss.}
\end{aligned} \tag{5}$$

For our purposes it is convenient to introduce a moving reference frame as $\xi=x-\int_{t_0}^{t}dt'v(t')$ into Eq. (4),

$$\partial_t\vec{u}-v\,\partial_\xi\vec{u}-\vec{w}|_{\vec{u}}=-\sum_i \delta_i\vec{P}_i x. \tag{6}$$

Assuming that the gradient perturbations are of the order of ϵ $(\epsilon\ll 1)$ and the field u and the velocity v scale as $\vec{u}=\vec{u}_0+\epsilon\vec{u}_1+\cdots$ and $v=\epsilon v_1+\cdots$, respectively, we get in the first order expansion of Eq. (6)

$$-v_1\partial_x\vec{u}_0-\partial_u\vec{w}|_{\vec{u}_0}u_1=-\sum_i \delta_i\vec{P}_i x, \tag{7}$$

where $\partial_u\vec{w}|_{\vec{u}_0}$ is the Jacobian of the linearized problem of Eq. (6). The solvability condition for Eq. (7) gives

$$v_1=\sum_i \delta_i\frac{\langle\vec{a}_0|\vec{P}_i x\rangle}{\langle\vec{a}_0|\partial_x u_0\rangle}\equiv\sum_i \delta_i\beta_i, \tag{8}$$

where $\vec{a}_0$ is the null vector of the adjoint Jacobian $\partial_u\vec{w}^+|_{\vec{u}_0}$ $(\partial_u\vec{w}^+|_{\vec{u}_0}\vec{a}_0=0)$. Similar to the case of phase gradients the velocity of the soliton is proportional to the applied gradient. Due to the lack of second order time derivatives in the evolution [Eqs. (1)] the soliton has no effective mass and does not need time for acceleration. It instantaneously responds to the changes in the system parameters. Generalizing Eq. (8) for two transverse dimensions we can write the following expression for a two-dimensional evolution of the soliton center:

$$\frac{d\mathbf{r}_\perp}{dt} = -2\nabla_\perp \phi + \beta_E \nabla_\perp |E| + \beta_{\gamma_A} \nabla_\perp \gamma_A + \beta_{\gamma_B} \nabla_\perp \gamma_B + \beta_{\Delta_A} \nabla_\perp \Delta_A + \beta_{\Delta_B} \nabla_\perp \Delta_B . \quad (9)$$

Here $\mathbf{r}_\perp = (x,y)^T$, $\nabla_\perp = (\partial_x, \partial_y)^T$, and $E = |E(\mathbf{r}_\perp)| e^{-i\phi(\mathbf{r}_\perp)}$, $\gamma_{A,B} = \gamma_{A,B}(\mathbf{r}_\perp)$, and $\Delta_{A,B} = \Delta_{A,B}(\mathbf{r}_\perp)$ are functions of $\mathbf{r}_\perp$. The first term on the right-hand side of Eq. (9) is due to the effect of a local phase tilt of the holding field and its analog can be found in Eqs. (3). The next term (coefficient β_E) describes the inhomogeneity of the intensity of the holding field, which is unavoidable for realistic pump profiles. The coefficients β_{γ_A} and β_{γ_B} describe the effect of varying losses of the cavity due, e.g., to an inhomogeneous reflectivity of the mirrors. The last two terms (coefficients β_{Δ_A} and β_{Δ_B}) account for a varying detuning at FF and SH frequencies, which can be induced by transverse variations of the cavity length due, e.g., to curved mirrors.

The coefficients in Eq. (9) can be determined numerically by solving Eqs. (1) or semianalytically by using the derivation presented above Eq. (8). In any case we found excellent agreement between the results of both methods. The dependence of the dimensionless coefficients β_E on the input field E for the one-dimensional soliton is shown in Fig. 3. Vertical dashed straight lines indicate the boundaries of the cw hysteresis loop. The sign of the coefficients gives an idea of the dynamical response of the cavity soliton. It turns out that the soliton tends to move into the area of the cavity where the system is closest to resonance.

We found β_{Δ_A} and β_{Δ_B} to be positive in the whole parameter domain (see Fig. 3). The intuitive explanation of this finding is based on the fact that cavity solitons exist only if both detunings are negative. While moving towards increasing detunings the soliton approaches the resonance. This has the important consequence that for a stable cavity with concave mirrors solitons tend to move to the central axis of the cavity. Hence they stay in the excited area and remain stable.

For an inhomogeneous intensity of the holding beam the response of the cavity soliton is more involved. For one- and two-dimensional solitons (see Figs. 3 and 4) the coefficient β_E can change from positive to negative values at a certain value of the input field $E = E_s$. Again this behavior can be explained by the tendency of the soliton to approach the resonance. If the input field is below E_s the nonlinearly induced phase shift drives the system closer to resonance conditions. In contrast for $E > E_s$ the soliton has already passed the resonance and tends to reduce the actual intensity. Consequently this change of sign happens for much lower intensities in the two-dimensional case, because the field enhancement at the center of that cavity soliton is much stronger. The last picture of Fig. 3 illustrates that there is also a fixed point in the case when a gradient exists in γ_A.

Let us talk about the consequences of this finding in more detail. For local input fields below E_s the soliton moves into areas with higher irradiance, whereas for fields above E_s this tendency is inverted. Finally all cavity solitons concentrate at lines or points with the local holding field E_s. Starting with a bell-shaped excitation with a maximum holding field less than E_s any soliton will climb to the top of the beam. While increasing the holding field above E_s the soliton will leave the central position. Increasing the peak power of the holding beam above the upper limit point of the hysteresis loop [see Fig. 2(a)] causes a spontaneous destabilization of the top of the beam. The evolving pattern periodically emits CSs to the wings of the beam (see Fig. 5). Those CSs climb down the slope of the beam until they reach a holding beam intensity

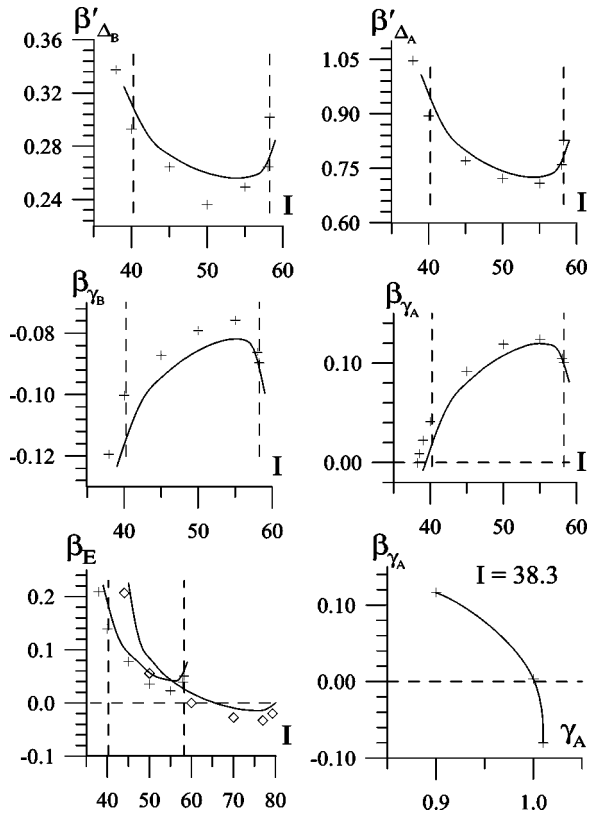

FIG. 3. Coefficients determining the dynamical response of a one-dimensional CS to linear variations of different system parameters for $\gamma_A = 1$, $\gamma_B = 0.6$, and $\Delta_A = -4$. The solid lines refer to semianalytical results based on Eq. (8), the symbols result from the numerical solution of the evolution equations (1) for $\Delta_B = -5$ (crosses) and $\Delta_B = -7$ (rhombs).

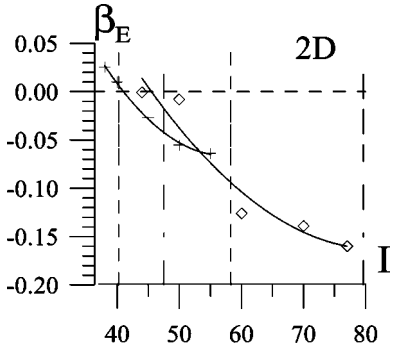

FIG. 4. Coefficient determining the dynamical response of a two-dimensional CS to linear variations of the intensity of the holding beam for $\gamma_A = 1$, $\gamma_B = 0.6$, $\Delta_A = -4$, and $\Delta_B = -5$ (crosses), $\Delta_B = -7$ (rhombs).

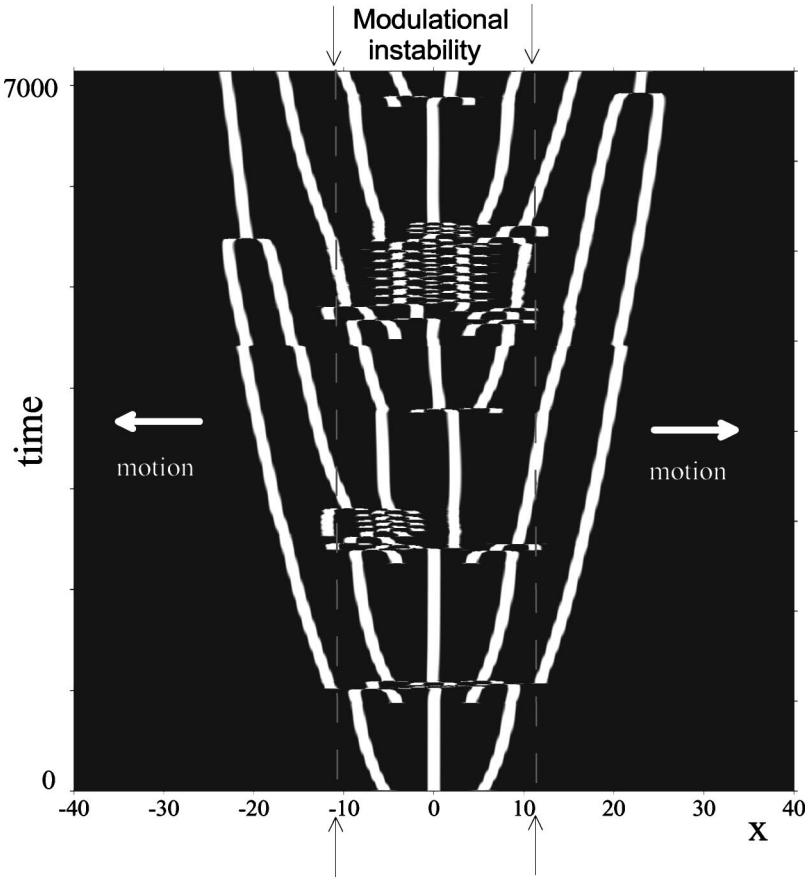

FIG. 5. Generation, motion, and decay of CSs on a holding beam with a peak amplitude above the upper limit point of the hysteresis loop for $\gamma_A=1$, $\gamma_B=0.6$, $\Delta_A=-4$, and $\Delta_B=-5$. The intensity decreases from $I=90$ at the center to $I=45$ at the boundary linearly. The modulational instability sets in at $I=79.63$.

I_s. At this point the CSs stop and fuse with other solitary waves generated before. Hence an intensity gradient can be used to generate and to eliminate CSs in all-optical processing schemes.

It is clear that in the vicinity of the fixed point the soliton should have a negative acceleration. Therefore, the previous asymptotic approach giving a constant value of the velocity should be modified, if the input field is sufficiently close to E_s. Let us assume that $E=E_0+\delta_E x$ and $|E_s-E_0|\sim\delta_E$. The position of the soliton center x_0 is an adiabatic function of the time and $\partial_t x_0\sim\delta_E^2$ is the soliton velocity. Substituting expansion $\vec{u}=\vec{u}_0+\delta_E\vec{u}_1+\delta_E^2\vec{u}_2+\cdots$ into Eqs. (1) and switching into the frame linked to the soliton center $\xi=x-x_0$ we find

$$
\begin{aligned}
&-\partial_u\vec{w}(\epsilon\vec{u}_1+\epsilon^2\vec{u}_2)\\
&\quad=\dot{x}_0\partial_x\vec{u}_0-\delta_E(\xi+x_0)\vec{P}_E\\
&\qquad+\delta_E^2[x_0^2\vec{n}_2(\xi)+x_0\vec{n}_1(\xi)+\vec{n}_0(\xi)]+O(\epsilon^3).
\end{aligned}
\tag{10}
$$

Vectors $\vec{n}_{0,1,2}$ appear due to nonlinear terms of the second order and it can be shown that $\vec{n}_{0,2}(\xi)$ are even functions of ξ. Multiplying the right-hand side of Eq. (10) by $\vec{\alpha}_0$ we find

$$
\dot{x}\langle\vec{\alpha}_0|\partial_x\vec{u}_0\rangle=\delta_E\langle\vec{a}_0|\xi\vec{P}_E\rangle-\delta_E^2x_0\langle\vec{a}_0|\vec{n}_1\rangle. \tag{11}
$$

Equation (11) shows that in the vicinity of the $E=E_s$ velocity of the soliton is a quadratic function of the gradient, while distance d of the soliton equilibrium position from the origin $(x=0)$ is inversely proportional to the gradient δ_E. Assuming without restriction of generality that initial position of the soliton was at the origin and the strength of the pump at this point was E_i, we find, from the elementary geometrical consideration, that $d=(E_s-E_i)/\delta_E$. On the other hand, Eq. (11) gives $d=\langle\vec{a}_0|\xi\vec{P}_E\rangle/(\delta_E\langle\vec{a}_0|\vec{n}_1\rangle)$. Comparing the two above expressions, we eliminated term containing $\vec{n}_1$ from Eq. (11) and find

$$
v=\left(1-\frac{x_0\delta_E}{E_s-E_i}\right)\frac{\delta_E\langle\vec{a}_0|\xi\vec{P}_E\rangle}{\langle\vec{a}_0|\partial_x\vec{u}_0\rangle}. \tag{12}
$$

Thus the difference of the modified expression for velocity (12) to Eq. (8) is a prefactor linearly depending on x_0.

B. Small scale perturbations: Fourier decomposition

The analysis of linear perturbations gives a good estimate of the response of CSs to long range fluctuations of the system parameters, which can be locally approximated by a linear expansion. However, there are a lot of perturbations with a spatial scale, which is small compared with the size of the CS. For instance, the mirrors of the resonator exhibit a certain roughness, which may considerably influence the dynamics of the nonlinear structures. Here we concentrate on the detuning, which is primarily influenced by fluctuating

properties of the mirrors. Those small scale spatial variations cannot be approximated linearly, i.e., they are not gradient. They are much better represented by a Fourier decomposition. Generally speaking, every random perturbation can be decomposed into a sum of harmonic functions of different frequencies. In what follows we investigate the response of the cavity soliton on a single harmonic modulation of a system parameter. To describe real random perturbations the same procedure has to be performed for each Fourier component separately. Here we investigate the response of the CS to the joint action of a short scale harmonic variation of the detuning and a linear increase of the holding beam intensity. Similar results can be easily obtained for perturbations of other system parameters.

We assume a periodic fluctuation of the detunings $\Delta_A \sim \Delta_B \sim \cos[k(x-x')]$ and a gradient perturbation of the incident intensity in the x- direction. For this situation the basic equation is

$$\partial_t \vec{u} - \partial_t x_0 \partial_\xi \vec{u} - \vec{w}|_{\vec{u}} = -\delta_E \vec{P}_E \xi - \delta_{\Delta_A} \vec{P}_A \cos[k(\xi + x_0)] - \delta_{\Delta_B} \vec{P}_B \cos[k(\xi + x_0)], \tag{13}$$

where x_0 is the soliton position. Let us first assume a vanishing gradient perturbation $\delta_E = 0$. The periodic perturbation consists of a sum of a symmetric and an antisymmetric contribution $\cos[k(\xi+x_0)] = \cos(kx_0)\cos(k\xi) - \sin(kx_0)\sin(k\xi)$. The antisymmetric contribution couples directly to the translational mode and thus causes a motion of the soliton. Only for $kx_0 = n\pi$ (n integer) the antisymmetric term vanishes and the soliton is at rest. In this case the cosine perturbation disturbs the soliton shape. The new soliton shape can be expressed in first order approximation as

$$\vec{u} = \vec{u}_0 + \sum_i \frac{\langle \vec{a}_i | (\delta_{\Delta_A} \vec{P}_A + \delta_{\Delta_B} \vec{P}_B) \cos(k\xi + n\pi) \rangle}{\lambda_i} \vec{e}_i ,$$

where λ_i are the eigenvalues of the symmetric eigenvectors $\vec{e}_i$ with $\partial_u \vec{w}|_{\vec{u}_0} \vec{e}_i = \lambda_i \vec{e}_i$ and $\vec{a}_i$ are the eigenvectors of the corresponding adjoint problem $\partial_u \vec{w}^+|_{\vec{u}_0} \vec{a}_i = \lambda_i^* \vec{a}_i$. The expression shows that only those eigenvectors $\vec{e}_i$ with a small amount of the corresponding eigenvalue λ_i contribute mainly to the changes of the soliton shape. Especially, close to the limit point of the soliton hysteresis, where one eigenvalue λ_1 of a symmetric eigenvector $\vec{e}_1$ passes through zero, the changes of the soliton shape may become huge. In this situation the soliton is deformed mainly in the direction of the eigenvector $\vec{e}_1$:

$$\vec{u} = \vec{u}_0 + \frac{\langle \vec{a}_1 | (\delta_{\Delta_A} \vec{P}_A + \delta_{\Delta_B} \vec{P}_B) \cos(k\xi + n\pi) \rangle}{\lambda_1} \vec{e}_1 .$$

Because the translational symmetry of the system is broken by the periodic perturbation a new nontrivial eigenvector arises from the original translational mode, i.e., the perturbation shifts the eigenvalue of the former translational mode from $\lambda_0 = 0$ to

$$\lambda_0 = \frac{\langle \vec{a}_1 | (\delta_{\Delta_A} \vec{P}_A + \delta_{\Delta_B} \vec{P}_B) \cos(k\xi + n\pi) \rangle \langle \vec{a}_0 | \partial_u^2 \vec{w}|_{\vec{u}_0} (\vec{e}_1) \partial_x \vec{u}_0 \rangle}{\lambda_1} . \tag{14}$$

For all positions $n\pi$ of the soliton the eigenvalue λ_0 has the same magnitude, but its sign variation is different for even and odd values of n (first term in the nominator). Therefore the discrete set of solitons can be classified into stable and unstable ones. If the oscillation period $2\pi/k$ of the perturbation becomes small compared with the soliton width (corresponds approximately to the width of $\vec{a}_1$) the first term in the nominator of Eq. (14) gets small too. Consequently the eigenvalues λ_0 tend to degenerate again. Now we additionally include the linear perturbation of the incident intensity $\delta_E \neq 0$. In the first order approximation of Eq. (13) we get the following differential equation for the soliton position x_0:

$$\partial_t x_0 = p - q \sin(kx_0), \tag{15}$$

where $p = \delta_E \langle \vec{a}_0 | \vec{P}_E \xi \rangle / \langle \vec{a}_0 | \partial_\xi \vec{u}_0 \rangle$ and $q = \langle \vec{a}_0 | (\delta_{\Delta_A} \vec{P}_{\Delta_A} + \delta_{\Delta_B} \vec{P}_{\Delta_B}) \sin(k\xi) \rangle$. Equation (15) can be solved analytically with two different scenarios arising. For a gradient perturbation $|p| < |q|$ the dynamics is described by

$$t - t_0 = \frac{k}{\sqrt{q^2 - p^2}} \ln\left(\frac{p \tan(kx_0/2) - q - \sqrt{q^2 - p^2}}{p \tan(kx_0/2) - q + \sqrt{q^2 - p^2}} \right), \tag{16}$$

where t_0 is an integration constant. Hence, the soliton reaches a stable fixpoint and remains trapped [see Fig. 6(a)]. In contrast if the inclination of the input intensity is large enough, $|p| > |q|$, the soliton follows the gradient [see Fig. 6(b)] with a velocity periodically changing as

$$t - t_0 = \frac{2k}{\sqrt{p^2 - q^2}} \arctan\left(\frac{p \tan(kx_0/2) - q}{\sqrt{p^2 - q^2}} \right). \tag{17}$$

A similiar trapping phenomenon was observed for patterns with a inclined mirror in single mirror feedback experiments in a sodium vapor cell [44].

V. EFFECTS OF WEAKLY DAMPED MODES

Until now we have concentrated on changes in the soliton speed, which are induced by a coupling of perturbations to

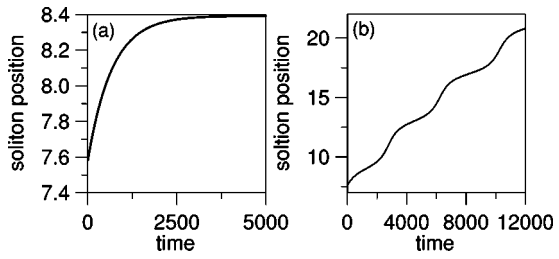

FIG. 6. Motion of a CS on a spatially periodic modulation of the cavity detuning under the action of a superimposed linear intensity gradient for $\gamma_A=1$, $\gamma_B=0.6$, $\Delta_A=-4$, $\Delta_B=-5$, and $I=42.5$. (a) The position of the CS vs time for a small linear gradient, where the CS is locked (amplitude of cosine modulation of both detunings $\beta_{\Delta_A}=\beta_{\Delta_B}=0.001$, gradient of the holding beam $\beta_E=0.015$). (b) The position of the CS vs. time for a large linear gradient, where the CS moves (amplitude of cosine modulation of both detunings $\beta_{\Delta_A}=\beta_{\Delta_B}=0.001$, gradient of the holding beam $\beta_E=0.005$).

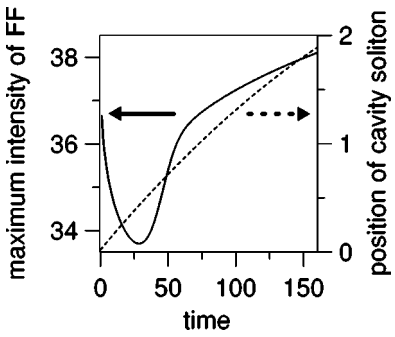

FIG. 7. Excitation of a CS for a holding beam intensity outside the domain of existence of CSs for $\gamma_A=1$, $\gamma_B=0.6$, $\Delta_A=-4$, $\Delta_B=-5$, and $E=6.18$ (limit point at around $E=6.2$). The applied gradient shifts the emerging structure towards higher intensities, where stable CSs exist.

the translational mode. However, the soliton possesses many additional nontrivial localized internal modes. The strength of the coupling of the perturbations to these modes is inverse to the respective eigenvalue and proportional to its overlap with the perturbation [25]. Because the most weakly damped internal mode is usually symmetric its overlap with the gradient perturbation vanishes. Therefore variations of the shape of the soliton due to external gradients are less pronounced. We have to expand up to second order to identify their consequences. Here we investigate the influence of a gradient perturbation close to a limit point of a soliton hysteresis where the eigenvalue λ_1 of a symmetric nontrivial eigenmode $\vec{e}_1$ passes through zero. For the sake of simplicity we restrict ourselves to an inclination of the input field around the critical point E_0 as $E=E_0+\epsilon\delta_E x+\epsilon^2 E_2$, where E_2 is a measure for the distance from the critical point and serves as the control parameter. The field scales like $\vec{u}=\vec{u}_0+\epsilon\vec{u}_1+\epsilon^2\vec{u}_2+\cdots$. As above the solvability condition at the first order leads to the soliton velocity. But additionally we have to take into account the symmetric mode $\vec{e}_1$. Therefore the field at order ϵ is $\vec{u}_1=C\vec{\nu}+B\vec{e}_1$, where $\vec{\nu}$ is given by

$$\partial_u\vec{w}|_{\vec{u}_0}(\vec{\nu})=\vec{P}_E x-\partial_x\vec{u}_0\langle\vec{a}_0|\vec{P}_E x\rangle/\langle\vec{a}_0|\partial_x u_0\rangle$$

and the amplitude C is equal to the input field inclination δ_E and B. In the stationary limit the amplitude B is determined at order ϵ^2,

$$B=\delta_E\frac{\langle\vec{a}_0|\vec{P}_E x\rangle\langle\vec{a}_1|\vec{e}_1\rangle}{2\langle\vec{a}_0|\partial_x\vec{u}_0\rangle\langle\vec{a}_1|\partial_u\vec{w}|_{\vec{u}_0}(\vec{e}_1,\vec{e}_1)\rangle}$$
$$\pm\sqrt{\delta_E^2\left(\frac{\langle\vec{a}_0|\vec{P}_E x\rangle^2\langle\vec{a}_1|\vec{e}_1\rangle^2}{4\langle\vec{a}_0|\partial_x\vec{u}_0\rangle^2\langle\vec{a}_1|\partial_u\vec{w}|_{\vec{u}_0}(\vec{e}_1,\vec{e}_1)\rangle^2}-\frac{\langle\vec{a}_1|\partial_u\vec{w}|_{\vec{u}_0}(\vec{\nu},\vec{\nu})\rangle}{\langle\vec{a}_1|\partial_u\vec{w}|_{\vec{u}_0}(\vec{e}_1,\vec{e}_1)\rangle}\right)+E_2\frac{\langle\vec{a}_1|\vec{P}_E\rangle}{\langle\vec{a}_1|\partial_u\vec{w}|_{\vec{u}_0}(\vec{e}_1,\vec{e}_1)\rangle}}. \quad (18)$$

Equation (18) shows that the soliton hysteresis is shifted due to an inclination of the input field δ_E with respect to the unperturbed case $\delta_E=0$, where

$$B=\pm\sqrt{E_2\frac{\langle\vec{a}_1|\vec{P}_E\rangle}{\langle\vec{a}_1|\partial_u\vec{w}|_{\vec{u}_0}(\vec{e}_1,\vec{e}_1)\rangle}}.$$

Thus attention has to be paid if applying the expression for the soliton velocity [Eq. (8)] close to the limit point of the soliton hysteresis. Equation (8) is only valid in the modified domain of existence of the solitons. Additionally, dynamical simulations show that the basin of attraction of solitons depends critically on the strength of the linear perturbation. For instance, an excitation of a soliton is even possible in front of the soliton hysteresis in certain parameter domains. An example is displayed in Fig. 7. First the excited spatial structure decays but additionally shifts in the direction of the gradient of the perturbation. After some time the domain of existence of the soliton is reached and a moving soliton arises that can be described by Eq. (8).

VI. SUMMARY

Using combined numerical and asymptotic techniques we have investigated the response of CSs on spatially dependent perturbations of the system parameters. In particular, we have established laws of motion for CSs in the presence of

linear and harmonic perturbations. For linear spatial variations of the input field we find critical values of the holding beam intensity, when the soliton rests in spite the presence of a inhomogeneous background field with no extrema. For a periodic perturbation superimposed on the linear gradient field we distinguished two cases, when soliton either gets trapped by the local field extremum of the periodic potential or moves along the gradient with oscillating velocity. We studied the soliton dynamics close to the boundary of its existence range, where the dynamics is determined by the interplay between the neutrally stable translational (asymmetric) and weakly stable symmetric modes of the soliton spectrum.

ACKNOWLEDGMENTS

S.F., D.M., U.P., C.E., N.R., and F.L. acknowledge the support of the European Community in the framework of the INTAS Grant No. 1997-581 and that of the Deutsche Forschungsgemeinschaft in the framework of the Grant No. 436 RUS 113/94/0 (R) and SFB 196. D.V.S. acknowledges support from the Royal Society of Edinburgh and U.K. EPSRC Grant No. GR/N19830.

[1] D.W.M. Laughlin, J.V. Moloney, and A.C. Newell, Phys. Rev. Lett. **51**, 75 (1983).
[2] N.N. Rosanov and G.V. Khodova, Opt. Spectrosc. **65**, 449 (1988); N.N. Rosanov, A.V. Fedorov, and G.V. Khodova, Phys. Status Solidi B **150**, 545 (1988).
[3] W.J. Firth and A.J. Scroggie, Phys. Rev. Lett. **76**, 1623 (1996).
[4] W.J. Firth and A. Lord, J. Mod. Opt. **43**, 1071 (1996).
[5] G.S. McDonald and W.J. Firth, J. Opt. Soc. Am. B **7**, 1328 (1990).
[6] M. Brambilla, L.A. Lugiato, and M. Stefani, Europhys. Lett. **49**, 2049 (1994).
[7] D. Michaelis, U. Peschel, and F. Lederer, Phys. Rev. A **56**, R3366 (1997).
[8] M. Brambilla, L.A. Lugiato, F. Prati, L. Spinelli, and W.J. Firth, Phys. Rev. Lett. **79**, 2042 (1997).
[9] M. Tlidi, P. Mandel, and R. Lefever, Phys. Rev. Lett. **73**, 640 (1994).
[10] R. Gallego, M. San Miguel, and R. Toral, Phys. Rev. E **61**, 2241 (2000).
[11] M. Kreuzer, A. Schreiber, and B. Thüring, Mol. Cryst. Liq. Cryst. **282**, 91 (1996).
[12] A. Schreiber, M. Kreuzer, and T. Tschudi, Opt. Commun. **136**, 415 (1997).
[13] M. Saffman, D. Montgomery, and D. Z. Anderson, Opt. Lett. **19**, 518 (1994).
[14] V.B. Taranenko, K. Staliunas, and C.O. Weiss, Phys. Rev. A **56**, 1582 (1997).
[15] G. Slekys, K. Staliunas, and C.O. Weiss, Opt. Commun. **149**, 113 (1998).
[16] V.B. Taranenko, K. Staliunas, and C.O. Weiss, Phys. Rev. Lett. **81**, 2236 (1998).
[17] V.B. Taranenko, I. Ganne, R.J. Kuszelewicz, and C.O. Weiss, Phys. Rev. A **61**, 063818 (2000).
[18] S. Barland, M. Giudici, J.R. Tredicce, L. Spinelli, G. Tissoni, L.A. Lugiato, and M. Brambilla, in *Nonlinear Guided Waves and Their Applications*, OSA Technical Digest (Optical Society of America, Washington, DC, 2001).
[19] P.L. Ramazza, S. Ducci, S. Boccaletti, and F.T. Arecchi, J. Opt. B: Quantum Semiclassical Opt. **2**, 339 (2000).
[20] B.A. Samson and M.A. Vorontsov, Phys. Rev. A **56**, 1621 (1997).
[21] B. Schäpers, M. Feldmann, T. Ackemann, and W. Lange, Phys. Rev. Lett. **85**, 748 (2000).
[22] W.J. Firth and G.K. Harkness, Asian J. Phys. **7**, 665 (1998).
[23] N.N. Rosanov and A.V. Fedorov, Opt. Spectrosc. **68**, 565 (1990).
[24] N.N. Rosanov, Opt. Spectrosc. **72**, 516 (1992).
[25] T. Maggipinto, M. Brambilla, G.K. Harkness, and W.J. Firth, Phys. Rev. E **62**, 8726 (2000).
[26] N.N. Rosanov, Opt. Spectrosc. **73**, 324 (1992); N.N. Rosanov, Proc. SPIE **1840**, 130 (1992).
[27] *Advanced Photonics with Second-Order Optically Nonlinear Processes*, edited by A.D. Boardman *et al.* (Kluwer, Dordrecht, 1998).
[28] C. Etrich, U. Peschel, and F. Lederer, Phys. Rev. Lett. **79**, 2454 (1997).
[29] U. Peschel, D. Michaelis, C. Etrich, and F. Lederer, Phys. Rev. E **58**, 2745 (1998).
[30] S. Longhi, Opt. Lett. **23**, 346 (1998).
[31] P. Lodahl and M. Saffman, Phys. Rev. A **60**, 3251 (1999).
[32] S. Longhi, Phys. Scr. **56**, 611 (1997).
[33] K. Staliunas and V.J. Sánchez-Morcillo, Phys. Rev. A **57**, 1454 (1998); K. Staliunas and V.J. Sánchez-Morcillo, Opt. Commun. **139**, 306 (1997).
[34] S. Trillo, M. Haelterman, and A. Sheppard, Opt. Lett. **22**, 970 (1997); T.N. Kutz *et al.*, J. Opt. Soc. Am. B **16**, 1936 (1999).
[35] G.L. Oppo, A. Scroggie, and W.J. Firth, J. Opt. B: Quantum Semiclassical Opt. **1**, 133 (1999).
[36] M. Le Berre *et al.*, J. Opt. B: Quantum Semiclassical Opt. **1**, 153 (1999).
[37] M. Tlidi, P. Mandel, and R. Lefever, Phys. Rev. Lett. **81**, 979 (1998); M. Tlidi *et al.*, Opt. Lett. **25**, 487 (2000).
[38] D.V. Skryabin, Phys. Rev. E **60**, R3508 (1999).
[39] D.V. Skryabin, A.R. Champneys, and W.J. Firth, Phys. Rev. Lett. **84**, 463 (2000).
[40] D.V. Skryabin and A.R. Champneys, Phys. Rev. E **63**, 066610 (2001).
[41] G.L. Oppo, M. Brambilla, and L. A. Lugiato, Phys. Rev. A **49**, 2028 (1994).
[42] P. Mandel, *Theoretical Problems in Cavity Nonlinear Optics* (Cambridge University Press, Cambridge, England, 1997).
[43] M. Tlidi, M. Le Berre, E. Ressayre, A. Tallet, L. Di Menza, Phys. Rev. A **61**, 043806 (2000).
[44] J.P. Seipenbusch, T. Ackemann, B. Schäpers, B. Berge, W. Lange, Phys. Rev. A **56**, R4401 (1997).